بسم الله الرحمن الرحيم

Sudan University of Science and Technology

Faculty of Engineering

Aeronautical EngineeringDepartment

Study of the Erosion in First Stage of Axial Flow Compressor

Thesis Submitted inPartial Fulfillment of the Requirements for the Degree of Bachelor of Science. (BSc Honor)

By:

1. EisaEsam Ali Ahmed
2. Khalid AbdelrahmanKhiderKhalifa
3. Mohammed Altayeb Ibrahim Ahmed

Supervised By:

A .prof: Ali AL Hussein Ahmed

الآيـــــــــــة

سورة البقرة الاية (102)

Abstract

Erosion is a process that describes continuous physical and chemical events which causes soil and rock on the earth's surface to loosen and move to a new location, the erosion occurred in first stage of compressor which is one of crucial component of gas turbine engine that leads to reduce performance of aircraft engine. This is a report of a research study about the mechanisms of erosive wear of first stage compressor blades in turbo shaft engines for helicopter aircrafts. Occurred defects for turboshaft engines in first stage compressor reduce blade thickness, reduce blade chord, increase surface roughness,increase close running clearance, making the blade structure weaker and cause losses in power and efficiency that lead to reduce life time of compressor.

NACA0012 airfoil had been tested in wind tunnel in two cases: clean and rough (to simulate erosion effect). The free stream velocity chosen to be constant to get the drag and lift coefficients, the results had been plotted in MATLAB. Results from MATLAB supported the theory that the erosion is affecting the forces and performance after comparing the results from two cases.

Suggestions made to coat the blade by chrome to increase the life time and fighting the effect of the ambient environment.

التجريد

التاكل هو عملية تشوة تحدث نتيجة للعوامل الفيزيائية والكيميائية علي التربة واالصخور والمواد الموجودة علي سطح الارض وتؤدي الي إضعاف خصائصهم . والتاكل او التعرية تحدث ايضا في محركات الطائرات والتي تعبر من اهم مكونات الطائرة و يكون أثر التاكل او التعرية واضح بشكل كبير علي ضاغط الهواء الموجود خلف مدخل الهواء بالنسبة للمحركات الطائرات العمودية لانها اكثر عرضه لعوامل البيئة من غيرها وبالتالي يضعف من كفاءة عمل الضاغط مما يضعف من كفاءة عمل المحرك و تقليل العمر الزمني له فتقل كفاءة اداء الطائرة تبعا للذلك.

ونحن في هذا البحث نقوم بدراسة علمية تأثير التاكل او التعرية علي الضاغط ولمعرفة مدي ضررها عليه وذلك باستخدم المعادلات النظرية وايضا بالاستعانة ببرنامج (ماتلاب) في عمل الحسابات اللازمة وتمثيلها في شكل منحنيات تؤكد النظريه المسبقه ان التآكل يؤثر علي العمر الزمني للمحرك وبالتالي كفاءة الطائره, ومن ثم نقوم بتحليلها و استنتاج الخلاصة و وايضا نقوم بإجراء تجربة إختبار عملية في معمل النفق الهوائي علي مقطع جناح متماثل في الحالة الاولي : يكون فيها سطح المقطع العلوي للجناح ناعم ونظيف وايضا في الحالة الثانيه :ان يكون السطح العلوي خشن واستخلاص قيم معدل الرفع ومعدل الكبح عند تثبيت السرعه علي قيمه معينه وتغيير زاوية الهجوم و ادخال القيم في برنامج الماتلاب لتمثيل التأثير بمنحنيات ودراستها وتحليلها ووضع الحلول المثلي لذلك.

ومن خلال الدراسه والبحث عن حلول وجد من الافضل طلاء الريشه بمادة الكروم لمقاومة التأثير البيئي وزيادة العمر الزمني للمحرك.

Acknowledgment

All thanks to Allah for helping us in accomplishing this research and also to people who made this project possible and good experience for us.

Wewould like to express our deepest thanks and sincere gratitude to oursupervisor **A. Prof. Ali Alhussien**who guided this work and helped whenever we was in need.

We also grateful to **wind tunnel lab technicians**for support us in experimental part.

Another special thanks totheengineer **Mohammed Balla**and the engineer **Mustafa Malik** and classmate the engineer **Mohammed Hassan**, for their assistance and help through period of this research.

Dedication

To the men whom learning us the life

Our fathers

To the women whose looks after us when we was a baby's

our dear mothers

To our dear martyrAhmed Albukhari Hamdto

To friends in patch 15

To greatest country of Sudan.

List of Contents

Contents

List of Figure

List of Tables

List of Symbols

C_L	Lift coefficient
C_D	Drag coefficient
CL/CD	Lift to drag ratio
E	erosion
E1	young modulus 1
E2	young modulus 2
F_{max}	Impact force
K1 K3 K12	constants
M	Mass of sand
q 1	Poisson's ration for sand 1
q 2	Poisson's ration for sand 2
R	radius of the particle
R_t	Tangential restitution ratio
Up	velocity of particle
V1	velocity of particle
Wd	Volume
ρ_p	Density of the particle
β1	impingement angle
β0	30 degree for ductile materials

Chapter One: Introduction

1.1 Overview

Sand erosion is a phenomenon whereby solid particles impinging on a wall cause serious mechanical damage to the wall surface.

Gas turbine engines for aircrafts and helicopters are subjected to severe erosion depending on design and operating conditions.

Erosion of compressor blades due to operation in particulate environments is a serious problem for the manufacturers and users of industrial and aeronautical gas turbines, because of drastic degradations in performance.

Erosion is affected by many factors such as the ingested particle characteristics, gas flowpath, blade geometry, operating conditions, and blade material.

Three major effects determine the performance deterioration of the compressor:

Increased tip clearances.

Changes in airfoil geometry.

Changes in airfoil surface quality

Figure 1 Helicopter in dusty area

1.2 Objectives

- Study of the mechanism of erosion of compressor rotor blades.
- Determine the erosion parameter as a function of particles velocity and impingement angle.
- Experimental study of the effect of blade surface roughness on the aerodynamic parameters

1.3 Problem Statement

- The intensity and pattern of erosion are dependent on the physical properties of particles, their sizes, concentration, velocities and angles of impingement, and the target geometry and material.
- The degradation in aerodynamic performance is mostly through deterioration of the optimized blade profile:
  - reduction in the blade chord;
  - blunting of the leading edge;
  - thinning of the trailing edge;
  - increase in tip clearance;
  - Increase in surface roughness.
- Erosion damage can lead to significant reduction in compressor pressure ratio, efficiency and stability margin.

1.4 Methodology

An intensive literature review had been done to collect data, in theoretical approach we considered the erosion as a function particle velocity and impingement angle also considering the impact force function in particle radius in addition to that the volume of erode part function in particle velocity.

In experiment theairfoil NACA 0012 chosen to be test model in wind tunnel, in first case of clean surface the values of the lift and drag at constant air speed of wind tunnel had been recorded and also for the second case of rough surface the values of lift and drag with constant wind tunnel airspeed had been recorded, then the values is processed in MATLAB and simulated in graphs, and then analysis regrading theoretical equations and that results was discussed and marked conclusion and reach to objectives report

1.5 Outlines of research

- Chapter one: introduction.
- Chapter two: literature review.
- Chapter three: calculations.
- Chapter four: results and discussion.
- Chapter five: conclusion and recommendations.

Chapter Two: Literature Review

2.1 Background

Erosion

Turbomachinery erosion is affected by many factors such as the ingested particle characteristics, gas flow path, blade geometry, operating conditions, and blade material. Both experimental and numerical studies were conducted to determine the pattern and intensity of compressor and turbine-blade erosion.

Grant and Tabakoff[14] and Balan and Tabakoff[15] conducted experimental studies of single stage axial-flow compressor erosion. Examination of disassembled rotor blades after sand ingestion revealed blunted leading edges, sharpened trailing edges, reduced blade chords, and increased pressure surface roughness. Sugano et al.

Reported similar observations regarding the changes produced by erosion in axial-induced draft fans of coal-fired boilers. They also determined that blade chord reduction and material removal from the pressure surface increased with particle size.

Richardson et al.presented results of JT9D high-pressure compressor diagnostic study in which they documented the changes in airfoil roughness, blade airfoil, and tip clearance with service. The study indicated that in general the changes correlated well with engine cycles not with hours of engine service.

Rotor-blade erosion was observed mainly in the outer 50% of the span, where significant reductions in the blade chord and thickness and changes in the leading- and trailing-edge geometries were observed. Surface roughness measurements indicated quick buildup with no trends observed beyond 2000 cycles. Tip clearances increased as a result of both blade shortening and rub strip erosion. Dunn et al.

Measured tip clearance that exceeded specifications by a factor of three with operation in dust-laden environments and reported surge occurrences when the engine was run in this deteriorated stat

Coating and Blade Material Erosion Studies and Facilities

Theoretical studies of material loss by solid particle erosion are predominantly empirical, involving basic assumptions as to the process governing material removal. Different combinations of cutting, fatigue, brittle fracture, and melting mechanisms have been proposed and supported by experimental data from erosion tests.

Experimental studies of particle surface impacts are necessary to particle-laden flow around the target to achieve the desired impactconditions over the tested coupons.

A testing method using a small jet of particle-laden air impacting a stationary specimen was used by (Finnie and late)r by other investigatorsfor measuring the erosion characteristics of materials. Photos of samples tested using this type of blast facility at different inclination angles are shown in Fig 2.

Large variationsin the depth and roughness of the tested surface can be seen in the figure. (Dosanjh and Humphry)performed a computational study of a particle-laden jet impinging normally on a flat wall. The results indicated significant radial variations in particle concentration, impact velocities, and impingement angle at the target surface.

The computed variations were strongly dependent on particle size and on the temperature and level of turbulence in the jet. Erosion wind tunnels control the particles' distribution and velocities in the test section and provide uniform particle impact conditions over the tested surface.In addition, the hot erosion tunnel developed by (Tabakoff and Wakeman),and shown schematically in Fig. 3, provides uniform high test-section temperatures for testing turbine blade materials and coating. Erosion tunnels also enable testing of actual vanes.

The results of erosion studies often express the ratio of surface mass or volume removal to impinging particle mass. In general the erosion rate of a given material is affected by the particles' impact velocity and impingement angle. The variation of erosion rate with impingement angle is characteristically different for ductile and brittle material as shown schematically in Fig. 4. This is attributed to the predominantly different mechanisms of cutting and brittle fracture. Typical variations of erosion rates with velocity and temperature are shown in Fig 5. Erosion rate is also affected by particle composition[31] and shape. Figure 6 shows

magnified scanning electron micrographs of fly ash, silica sand, and aluminum-oxide particles. The latter are most erosive because of their angular shapes and very sharp corners.

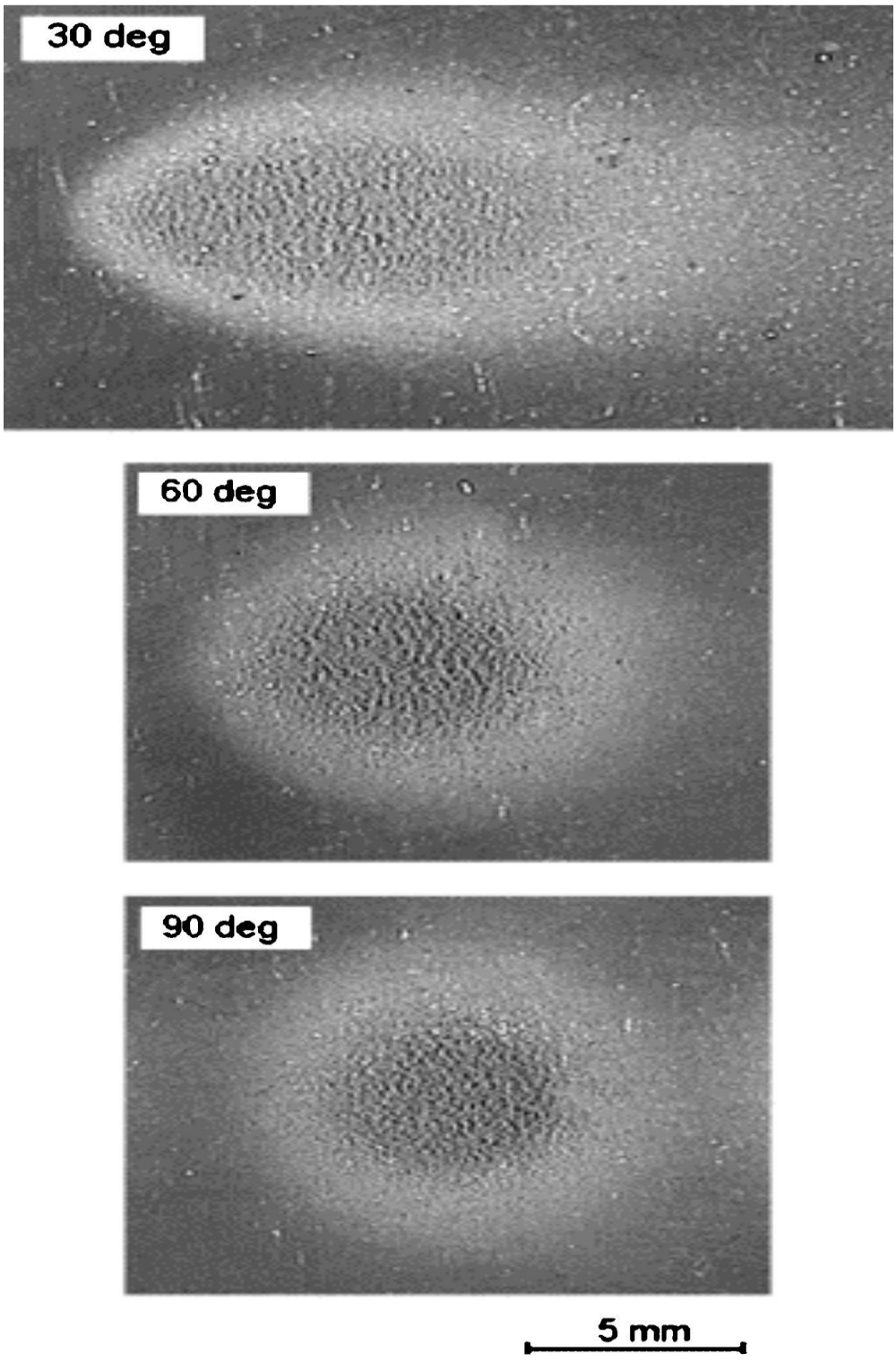

Figure 2: Samples tested in jet-blasted facility.22

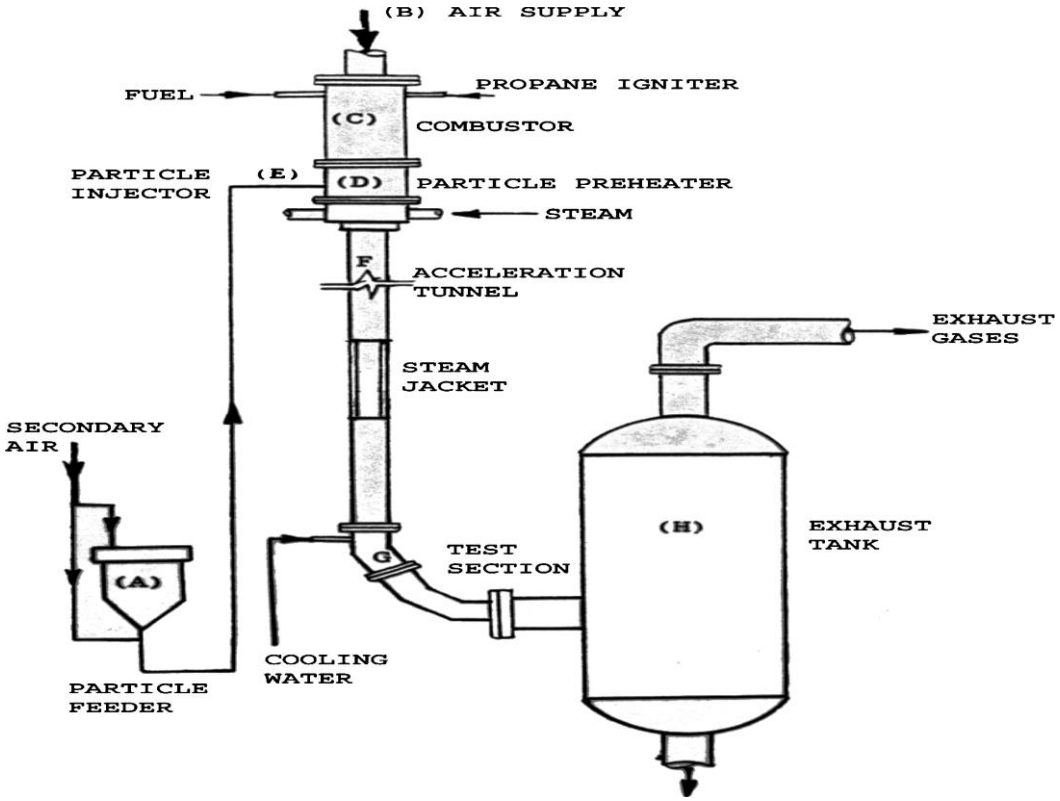

Figure 3: High-temperature erosion tunnel.

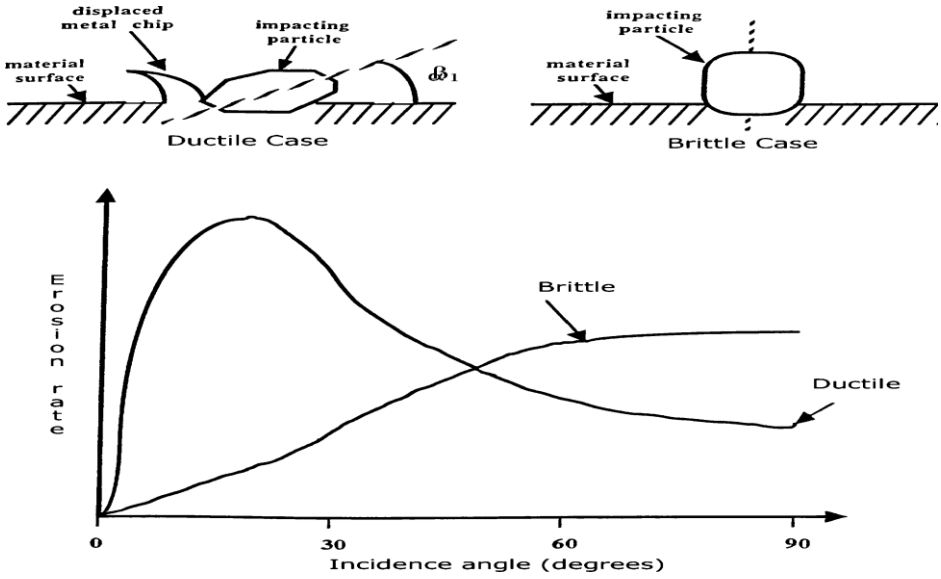

Figure 4: Erosion rate variation with impact angle.

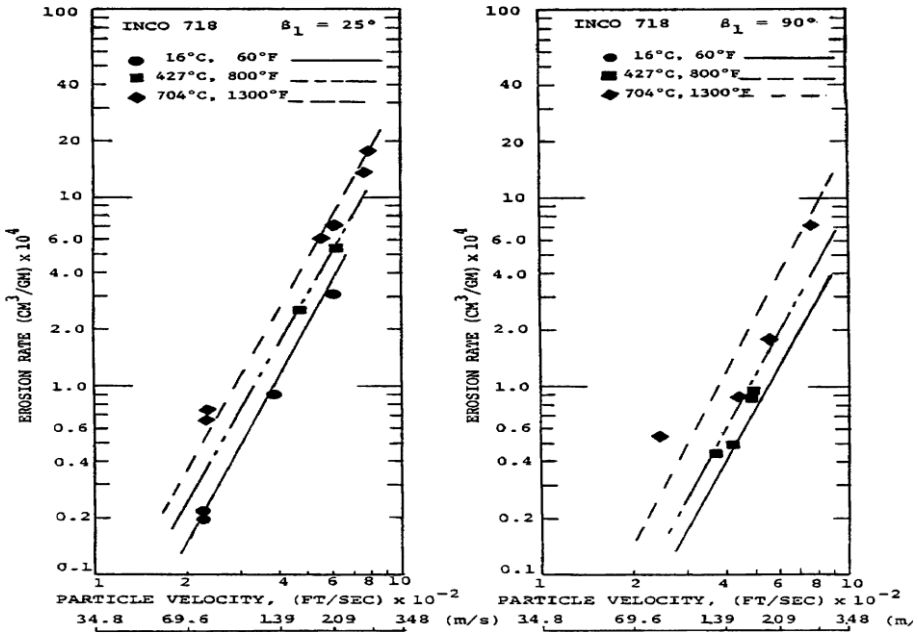

Figure 5: Erosion test results showing effects of temperature and impact

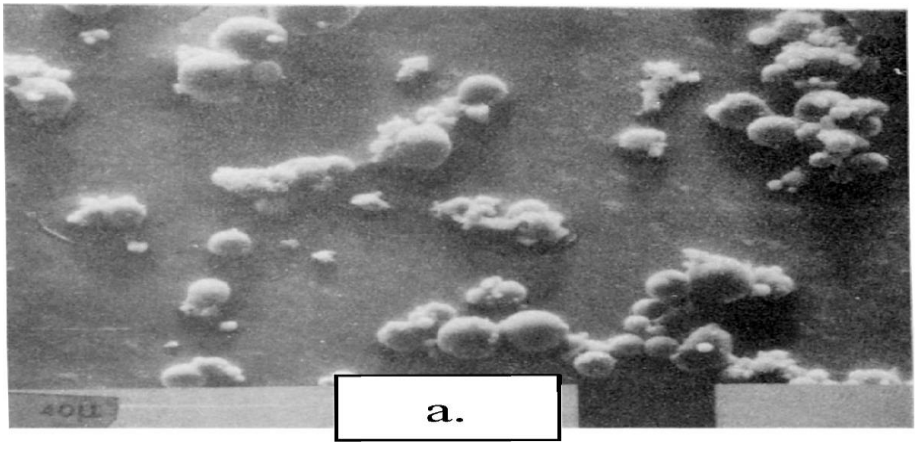

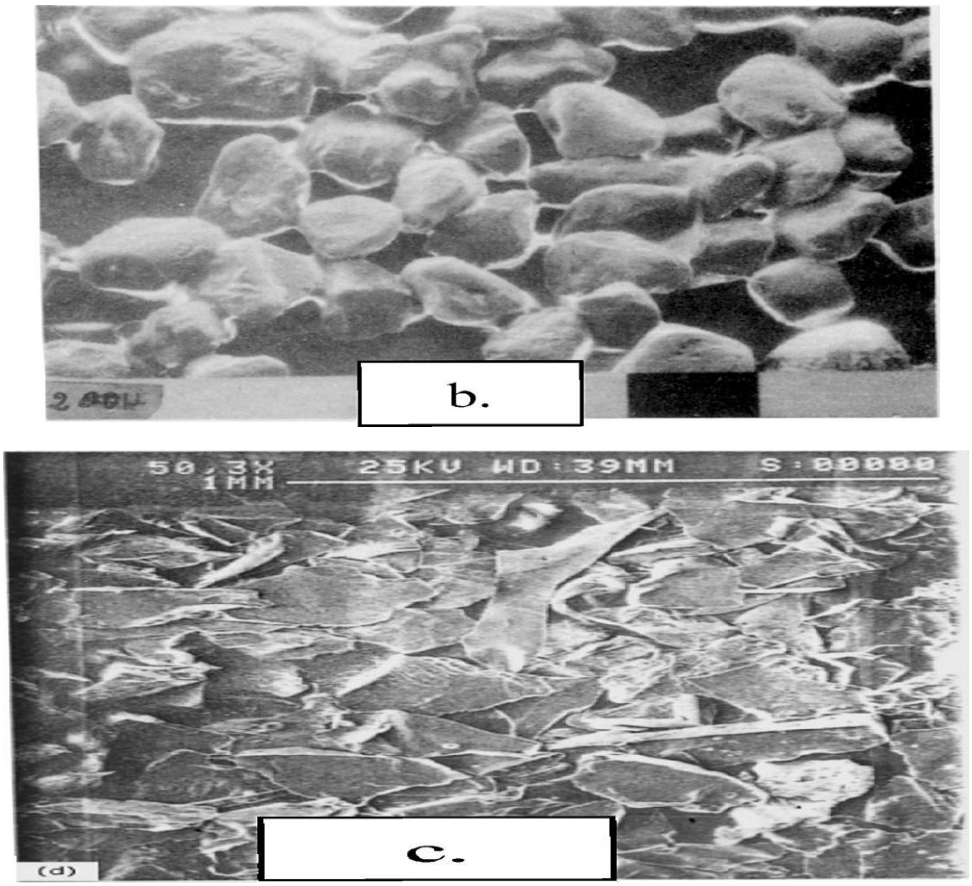

Figure 6: Electron micrographs of a) fly ash, b) silica sand, and c) aluminum-oxide particles.

Erosion test results obtained by (Grant and Tabakoff)using aluminum-oxide particles and by (Kotwal and Tabakoff)using alumina and silica particles of different sizes indicate that larger particles produced higher erosion rates, but that the effect of particle size on erosion rate diminished as impact velocity decreased.

Table 1 gives a list of some erosion tests with the blade coating materials and particles used in the tests, the test conditions, and the reference where the results were reported. Surface roughness characteristics were measured after erosion tests in some investigations.Surface roughness was found to correlate closely with the erosion rate in terms of variation with the impact angle, velocity, and particle size. The eroded surface roughness did not change beyond a certain limit even with additional mass removal by erosion. (Richardson) et al.also reported that compression system airfoil surface roughness did not change beyond 2000 cycles. Figure 7

clearly shows the difference between the roughness of the exposed and protected vane surfaces after being in the erosion tunnel.

In general, particles encounter repeated impacts with the turbine and compressor surface, and their trajectories are affected by the rebound conditions after each impact. Experimental studies have been conducted to measure the magnitude and direction of particle rebound velocity. Finnie[32] developed a system to measure particle velocities by tracking double-exposed pictures using a stroboscopic light source.

(Hussein and Tabakoff)used high-speed photography to investigate the rebound characteristics of particles from flat targets and to track actual particle trajectories in turbine cascades.(Wakeman and Tabakoff)used high-speed cameras for particle restitution measurements in the erosion wind tunnel, which was equipped with optical access through the test section.

Table 1: Wind-tunnel tests of blade materials and coating erosion

Substrate material	Coating	Impact (α), deg	Temperature, °C	Velocity, m/s	Particles	Reference
Cemented	Al_2O_3	0–90	260	140	Aluminum	2
Tungsten	T_iC	0–90	260	140	oxide	31
Carbide	T_iN	0–90	260	140	——	——
MAR 246	——	0–90	815	366	Fly ash	5
X-40	——	0–90	538	305	Fly ash	32
Inco 738	——	0–90	538	305	Fly ash	——
Cobalt	——	0–90	538	145–259	Fly ash	7
Rene 41	——	0–90	649	182–305	Fly ash	33
AM 355	——	0–90	316	122–305	Fly ash	——
Al 2024	——	0–90	Ambient	65–137	Fly ash	8
St St 304	——	0–90	Ambient	65–137	Fly ash	34
St St 304	——	0–90	Ambient	128	Quartz	——
St St 304	——	0–90	Ambient	122	Alumina	——
Ti 6A1-4V	——	0–90	Ambient	65–137	Ash	——
Al 2024	——	0–90	Ambient	92–152	Quartz	9, 35
MAR 246	T_iC	0–90	815	366	Fly ash	10
MAR 246	RT22	0–90	815	366	Fly ash	36
MAR 246	T_iC	0–90	815	305	Chromite	——
Ti-6-4	——	0–90	16–704	152	Aluminum oxide	13
Inco 718	——	0–90	16–704	152	Aluminum oxide	37
Steel 304	——	0–90	30–650	18–305	Aluminum oxide	——
Inco 600	——	0–90	371–493	100–300	Runway sand	14, 38
Waspaloy	Uncoated	0–90	538	305	Chromite	15
	T_iC	0–90	538	305	Chromite	39
Inco 738	——	0–90	482	183–305	——	16
FSX-414	——	0–90	482	183–305	Fly ash	40
X-40	——	0–90	482	183–305	——	——
St Steel 304	——	0–90	30–650	200–330	——	17
Rene 41	——	0–90	30–650	200–330	Fly ash	41
A286	——	0–90	30–650	200–330	——	——
St St 410	TiC	0–90	540	305	Chromite	18
INCO 718	Iron nitride	0–90	540	305	Chromite	42
St St 304	——	0–90	316, 650	120–300	Fly ash	19, 43
Ti-6A1-4V	Various multilayer coatings	0–90	Ambient	185	Aluminum oxide	20, 44
Inco 718	——	0–90	16–704	65–244	Quartz	21
Ti-6-4	——	0–90	16–704	65–244	Quartz	45
St St 355	——	0–90	Ambient—538	99–152	Silica	23
				122–305	Fly ash	46
St St 304	——	0–90	315–650	183–305	——	24
Rene 41	——	0–90	315–650	183–305	Ash	47
Ti-6-4	——	0–90	16–704	152	——	——
Inco 600	——	0–90	370–577	120–240	Quartz	25 48
St St 410	SDG-2207	0–90	565	305	Chromite	26
Inco 718	T_iC	0–90	538	305	Chromite	49
Waspaloy	T_iC	0–90	538	305	Chromite	——
WC	T_iC	0–90	Ambient—650	140	Chromite	——
WC	Al_2O_3	0–90	Ambient—650	140	Chromite	——
WC	T_iN	0–90	Ambient—650	140	Chromite	——
WC	Uncoated	0–90	Ambient—650	140	Chromite	——

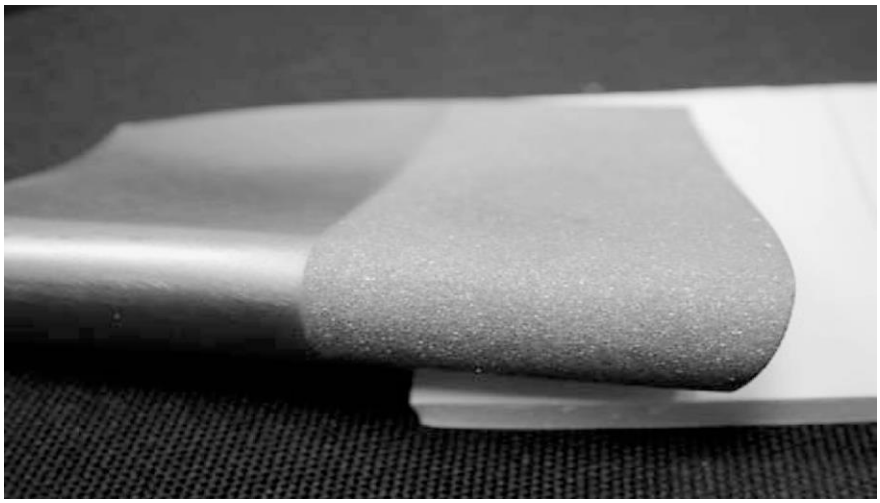

Figure 7: Vane surface roughness caused by erosion.

Because photographic methods were limited to particle sizes greater than 30 μ, (Tabakoff and Sugiyama)developed a method to use laser Doppler velocimetry (LDV) to measure fly-ash restitution characteristics. LDV was subsequently used in otherinvestigationsto measure the restitution characteristics for differentparticle material combinations. Figure 8 showstypical LDV results for the velocity and directional restitution ratios.

One can see that the restitution ratios exhibit variance around a mean value, which depends on the impact angle. The variance is likely associated with the orientation of non-rounded, particles at thetime of impact and with the erosion produced target surface irregularities. Particle rebound characteristics were found to be unaffected by the gas or target temperature.

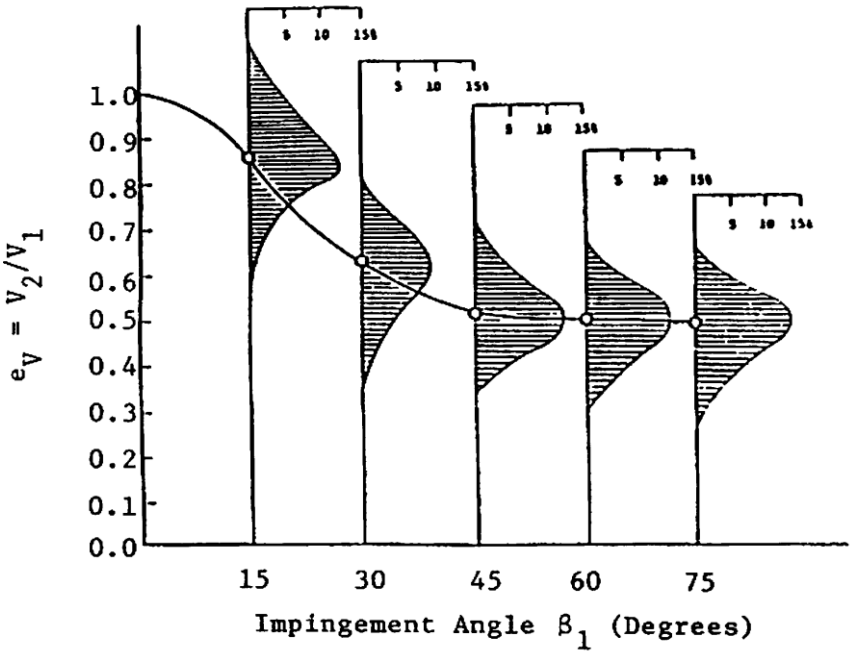

Figure 8: Typical LDV result for velocity and restitution ratios.

2.2 Study Mechanism of Erosion

2.2.1 Erosion Wear

Erosion of the solid particles is known as the process of material removal from the surface by the impingement of solid particles.[1]

2.2.2 Factors Affecting Erosion

The rate of material removal depends on the following parameters

1- Particle size

2- Velocity of impacting particle

3- Impact angle

4- Target material properties

5- Kinetic energy of impacting particle

6-Temperature effect

2.2.3 Particle Size Effect

Many contradicting theories have been reported in the literature about the particle size effect. Through work done by Finnie. [id it was reported that as the particle size decreased below 100 m) a dramatic decrease in the rate of erosion was noticed. Tilly and Sage[2]also studied the fragmentation behavior or irregular quartz particles, and the influence of particle size on the degree of fragmentation. They suggested that more impacts be required by small particles to remove a chip from a target, than that required by large particles.

2.2.4 Impact Angle

Erosion depend markedly on the angle of impingement. Finnie (1979) showed that three overlapping regions are involved.

1. At low angles (under of 20(degree)) of impingement the particles strike the surface, form a crater and then leave the surface. In some cases they remove a chip. In other cases they leave material piled up alongside and at end of the crater. This raised material is presumably removed relatively easily by subsequent particles.
2. At higher angles of between (20- 45 (degree)) the particles cut in to the surface and come to rest in the surface. Materials are piled up a head of the particle and again this pile up of material is vulnerable to removal by subsequent particles.
3. At still higher angles of (45-90 (deg.)) the particles generally ident rather than cut. In single impacts one can often see the original surface makings on the bottom of the crater.

2.2.5 Kinetic Energy of Particle

When a particle strikes a target, not all the kinetic energy of the particle is spent to form the crater on the target. The initial kinetic energy of the particle is partitioned for three different impact geometry's. For the spherical projectiles at normal impacts 1-10 % of the initial kinetic energy is restored to the particle by elastic forces. Most of the initial energy is dissipated in the target and the energy contained in the elastic wave field that cannot contribute to erosion may be estimated.[3] Hutchings suggested that this energy is about 1-5% of the initial energy having about 90% expended in plastic work.

Of this 90% up to 10% will be stored in the metal in dislocations and other crystal imperfections leaving 80% of the kinetic energy of the particle which is degraded into heat. At oblique impact angles rather less of the initial energy of the particle is expended in plastic work. D41 The work carried by Hutchings 1976 which indicates that for ploughing impact of a sphere at 30 angle, around 40% of the initial energy is available to form the indentation and hence to cause erosion. The case of angular impacting particles is more complex since the shape and orientation of the particle is important. Based on the work of Hutchings 1976 [4] demonstrated

that the rotational kinetic energy of the rebounding particle may be appreciable and that perhaps 40-80% of the initial kinetic energy is dissipated in plastic work.

2.2.6 Velocity of Impacting Particle

Investigations of the effect of velocity, have suggested that erosion can be related by:

$\Delta_{m\cdot}$ = constant * V^n Finnie suggested that the velocity exponent n has a value of 2, but a later work Finnie et al [15] gave n a value of about 3 and higher values have been reported for brittle materials. Hutchings found experimentally for steel spheres a value shows a typical curve for effect of velocity on different materials using different particle sizes.

2.2.7 The Target Material Properties

The material behavior is characterized by whether it is basically brits• or ductile. The relative behavior of the different materials also depends on the impact conditions. When comparing the relative performance of brittle and ductile material as shown in a brittle material may be more resistant to glancing impacts (at low impact angles), less resistant to normal impacts (higher impact angles). There can be a similar crossover in terms of particle size. For erosion at a glancing angle brittle material are more resistant to small particles but less resistant to large particles. Work carried out by Finnie, (Walks and Kabi)[5]relates erosion to the hardness of the target. They suggested that the volume removed is proportional to (1/ HV). Magee et al[6] interpreted the comparative erosion behavior of aluminum and steel and they found that aluminum is eroded more than steel for an impact angle of 30 (deg.) but for higher angles its erosion is smaller than of steel

2.2.8 Temperature Effect

As many components that are affected by erosion operate at high temperature. Some works have been done to investigate the effect of temper Lure on erosion. Tilly [17] reported that the erosion of mild steel decreased with increasing temperature to a round 400 C0 while 11%Cr steel

showed neat IN constant erosion with the increasing of temperature. Young and Ruff [18] have an experimental work to study, temperature Effect on erosion they work at 25 CI' &500c", with various velocities and impact angles over a wide range of particle sizes. And they determined that the relative weight loss.

2.2.9 Protection against Wear

Various techniques for providing surface protection to wear are as follows:

- Electro plating
- Anodizing
- Diffusion
- Metal spraying
- Hard facing

2.2.10 Electroplating

The wear resistance of a metal part can be improved by electroplating a harder metal on its surface. The metals most often plated on base materials are chromium, nickel, and rhodium. Two types of chromium plating used chromium and porous chromium. The hard-chromium plate is the same as that used for decorative purposes but much thicker, usually from 0.000254cm to 0.0254cm. Porous chromium plate has on its surface carefully controlled. The hardness of chromium plate is equivalent to 950 to 1050 Vickers. Another factor contributing to the reduction of wear is the low coefficient of friction of chromium plate. The high corrosion resistance of chromium is helpful in reducing wear under corrosive conditions. The hardness of nickel plate is from 140 to 425 Vickers depending upon the nickel — plating solution. Nickel plate is a good deal softer than Chromium plate, but in many, cases it is hard enough for the purpose and more economical. The hardness of rhodium plate is from 540 to 640 Vickers, and it is wear resistance is between those of nickel late and chromium plate. Rhodium plate has high reflectivity, high heat resistance.[7]

In addition to electroplating the nickel and chromium alloys are also used as alloying constituents with iron in stainless steel and with other metals such as copper. Nickel and chromium plate provide protection by the formation of an actual physical non corrosive harrier over steel. Electroplating particularly chromium on steel, are somewhat porous.

2.2.11 Surface Coatings

It was developed by PRAD (Russian Erosion Resistant Coatings for US Navy GTE Compressors) a new coating to protect the (TV2-117) engine compressor, which experienced sever erosion damage. This erosion resistant coating designed to prevent compressor erosion under operation in erosive media (sand, dust, and volcanic ash). The other designed goals are, corrosion resistance, and designed for environments.

2.2.12 Erosion Resistance Coating Description

Bond coat, Multi-layer using titanium nitrates, The thickness 5-20i/ m, Hardness 2800 — 3200 Vickers, Operating temperature range: 60 e to + 600 c°

2.2.13 The Coating Benefits

Operational Readiness,Longer on- wing time(less premature removal), Less down time of aircraft, Fewer spare engine required c. Lower repair and overhaul cost, Fewer shop visits, Lower cost of spare/replacement parts, Compressor components, including hot section components

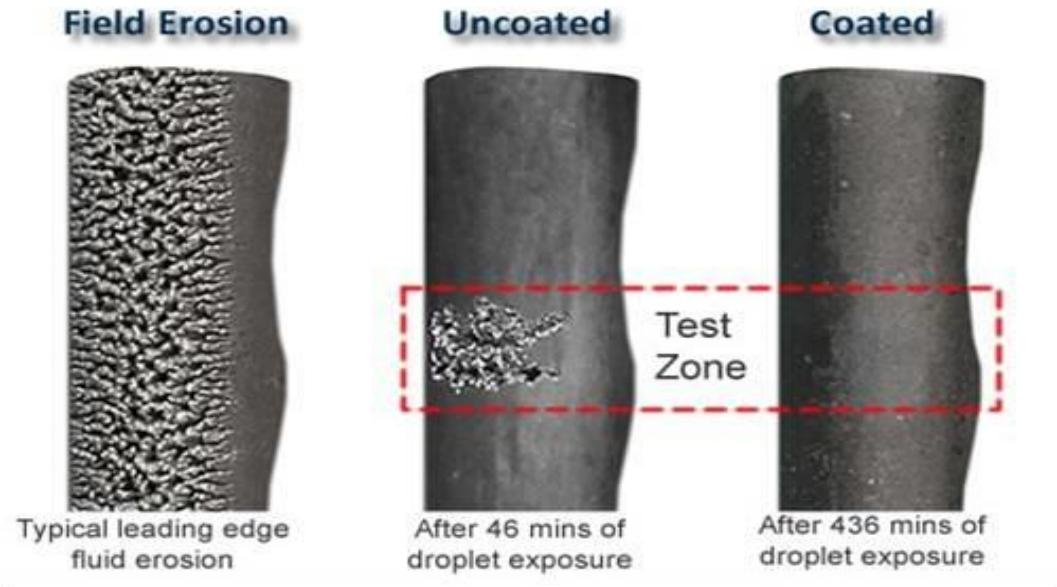

Figure 9 levels of blade coating

Table 2: Erosion Resistance Coating TV2-117 Service Performance

Description	Non-Coated	Coated
Rate of premature engine removal due to erosion	20-45%	0%
Rate of blades/vanes rejected due to erosion	70-80 %	2-3%(mostly due to FOD)
Engine performance debit at overhaul	10-30%	≤ 3 %

This coating had been examined and successful in more than one engine (TV2-117) which flying on MI-8 Helicopter and (TV3-117) which flying on MI-17, MI-24, M1-28, KA-32, KA-50, and KA-52 Helicopters.Comparison between the coated blades and the UN coated one, so the comparison give us the following benefits: * Safety and reliability increase of engine and aircraft. (a) Less increase in operating exhaust temperature (b) Less vibration degradation * Operational advantages[8].

Chapter Three: Calculationand Experimental

3.1 Calculation

Effect of erosion with impingement angle and velocity of particle, by using equation 1 below. Regarding table below, calculate by code in appendix A for the erosion with change for angle of attack at constant velocity of particle for air flow, and also calculate by code in appendix B for the erosion with change of impact for airflow velocity all calculation we are use MATLAB

$$\boldsymbol{E = K1 \left\{ 1 + CK \left[K12 * SIN\left(90 * \frac{B1}{B0}\right)\right]^2 \right\} V1\, COS^2\, B1(1 - Rt) + K3\, \{ V1\, SIN(B1)\}^4 \ldots} \quad \textbf{(1)}$$

And also calculation effect impact force with velocity of particle by equation below

$$Fmax = \left(\frac{20*\pi}{3} * \rho p\right)^{\frac{3}{5}} R^2 \left(\frac{1}{6*\left(\frac{1-q1^2}{E1}+\frac{1-q2^2}{E2}\right)}\right)^{\frac{2}{5}} Up^{\frac{6}{5}} \quad \text{..... (2)}$$

$$W_D = \frac{\frac{1}{2}*M*[V-K]\text{^}2}{\varepsilon} \quad \text{.....(3)}$$

3.2 Experimental Results

We are use in this experimental symmetric airfoil (0012) for clean surface to simulation blade compressor without erosion and record reads of parameters in table below.

Table 3: Reads of wind tunnel

α	CL1	CL2	CD1	CD2	CL1/CD1	CL2/CD2
-3	0.627	0.4375	0.0475	0.045	13.2	9.722222
-2	0.827	0.8125	0.02375	0.02625	34.82105	30.95238
-1	1.125	1.0625	0.0175	0.02125	64.28571	50
0	1.27	1.125	0.0175	0.0175	72.57143	64.28571
1	1.327	1.3125	0.01875	0.01625	70.77333	80.76923
2	1.53	1.4375	0.02	0.0175	76.5	82.14286
3	1.625	1.5	0.02125	0.01875	76.47059	80
4	1.75	1.625	0.022	0.02125	79.54545	76.47059
5	1.825	1.75	0.02375	0.02325	76.84211	75.26882
6	1.863	1.875	0.02625	0.025	70.97143	75
7	2	1.9375	0.02875	0.02625	69.56522	73.80952
8	2.125	2	0.03	0.02875	70.83333	69.56522
9	2.135	2.125	0.0325	0.0325	65.69231	65.38462
10	2.135	2.1875	0.03375	0.03625	63.25926	60.34483
11	2.125	2.21875	0.035	0.04375	60.71429	50.71429
12	2.118	2.234375	0.03875	0.04625	54.65806	48.31081

13	2.1	2.234375	0.05		42	
	2.095	2.21875				
	2.085	2.15625				
	2.05	2.0625				

Figure 10: New blade within wind tunnel

Figure 11: Blade within rough surface in the wind tunnel

Chapter Four: Results

4.1 Effect Erosion onImpingement Angle

MATLAB used to plotted graphs by appendix A

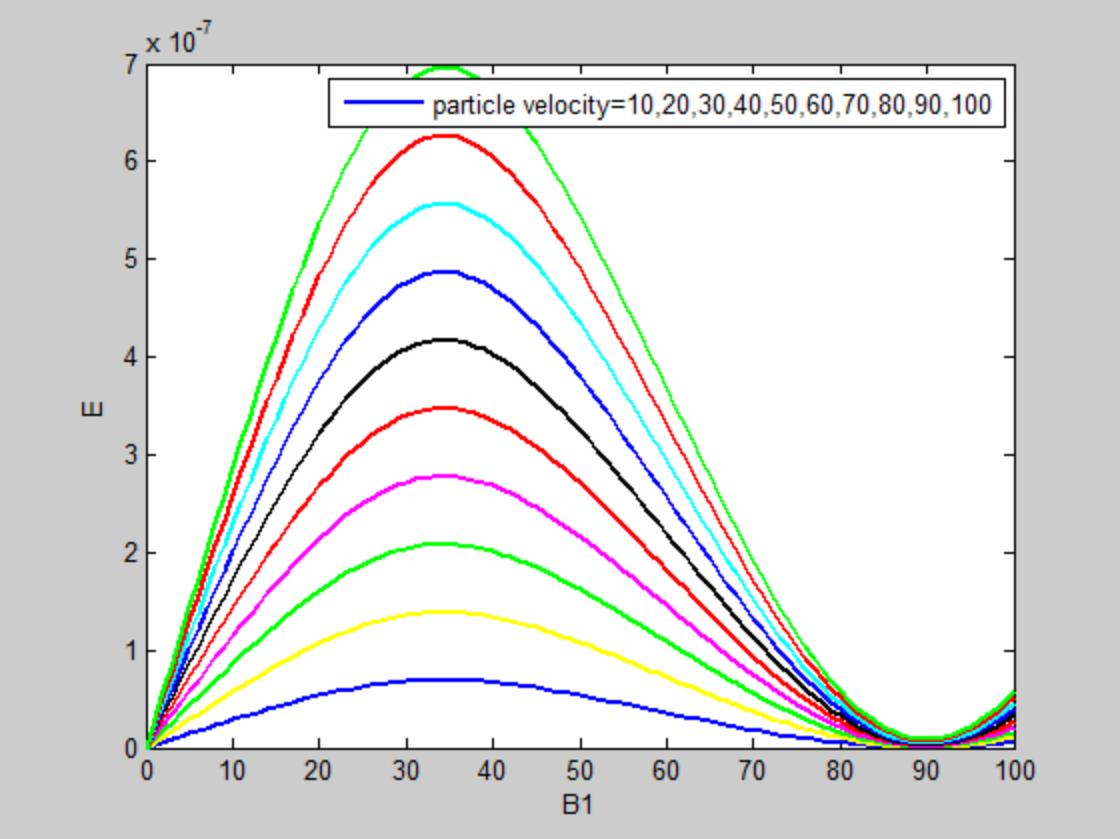

Figure 12: Effect of Impingement Angle on Erosion

4.1.1 Discussion Results Effect Impingement Angle on Erosion

We show in this figure relation between the erosion and impingement angle in x axis represent the impingement angle and y axis represent the erosion.

We see the curve begin from (0deg) increase linearly to reach (6.9*10^-8) in blue line and reach (1.39*10^-7) in yellow line and reach (2.2*10^-7) in green line and reach (2.8*10^-7) in magenta line and reach (3.5*10^-7) in red line and reach (4.2*10^-7) in black line and reach (4.8*10^-7) in blue line and reach (5.7*10^-7) in cyan (blue-green) line and reach (6.2*10^-7) in red line and reach (7*10^-7) in green line at angle (35 degree) and then we see the curve decreased until near zero at angle (90degree) of all figures.

4.2 Effect of Erosion on Impact Velocity

MATLAB use to plotted graphs by appendix B

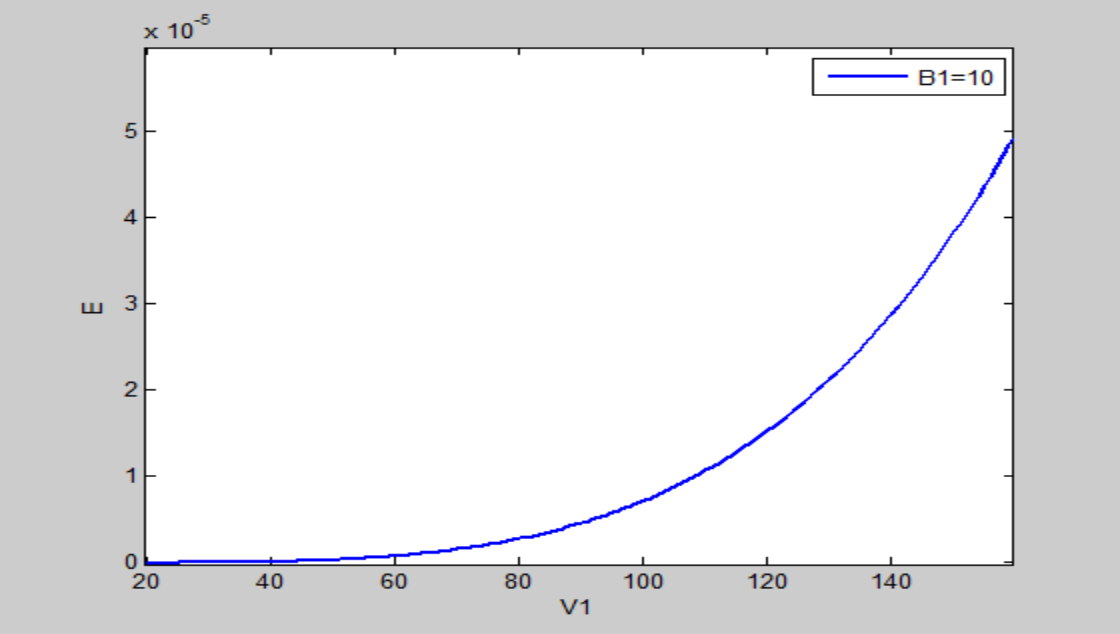

Figure 13: E vs V1 at B1 = 10

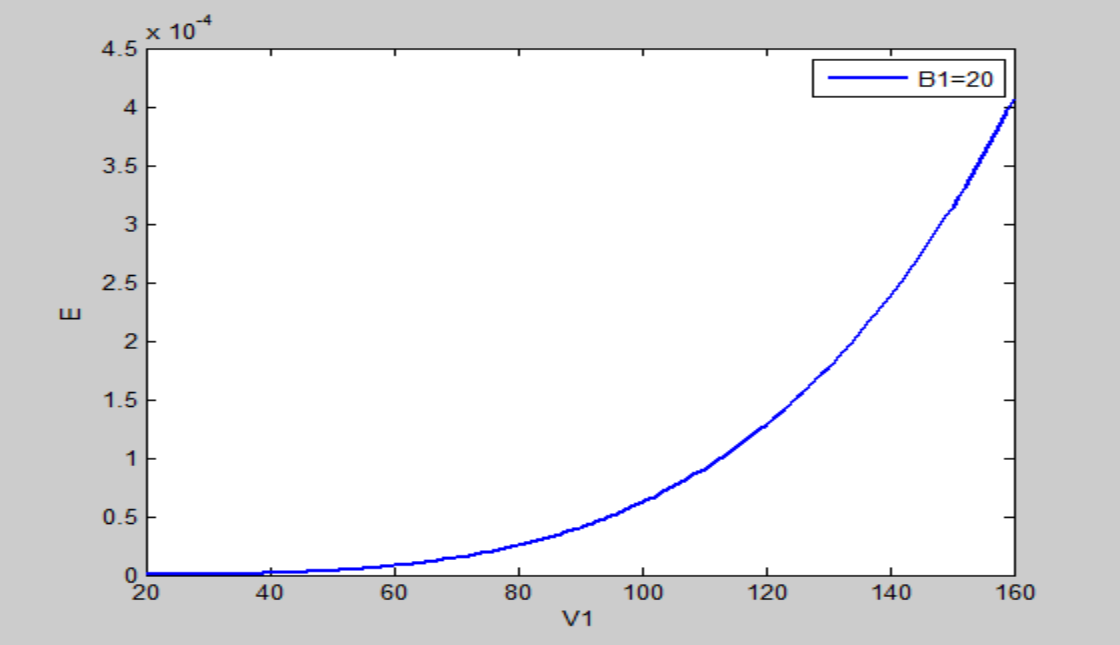

Figure 14: E vs V1 at B1 = 20

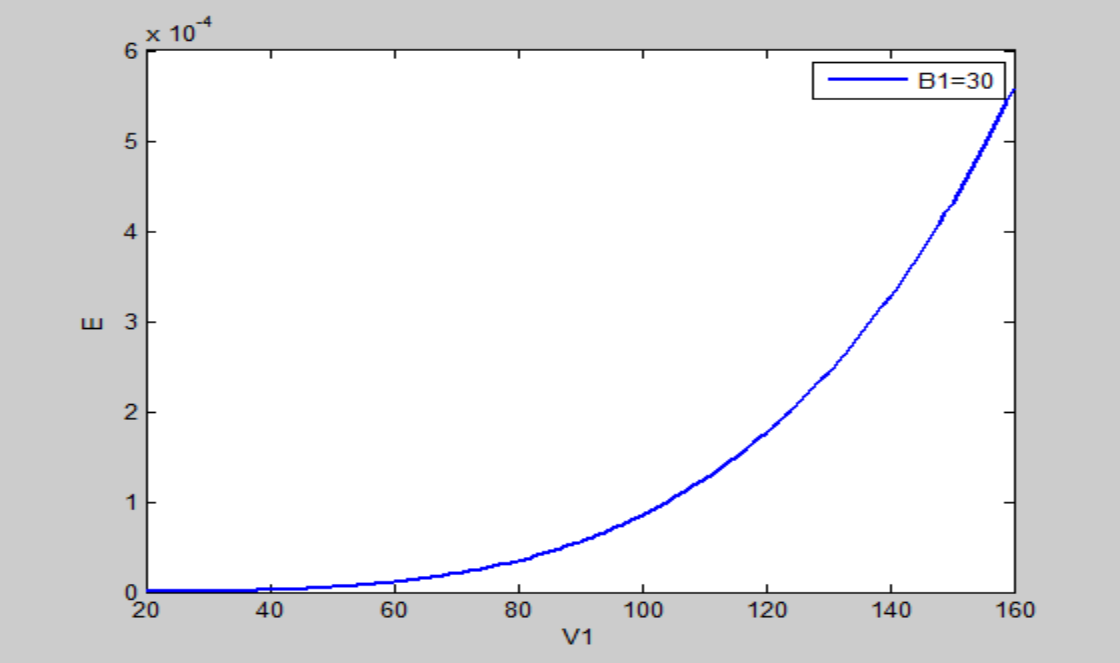

Figure 15: E vs V1 at B1 = 30

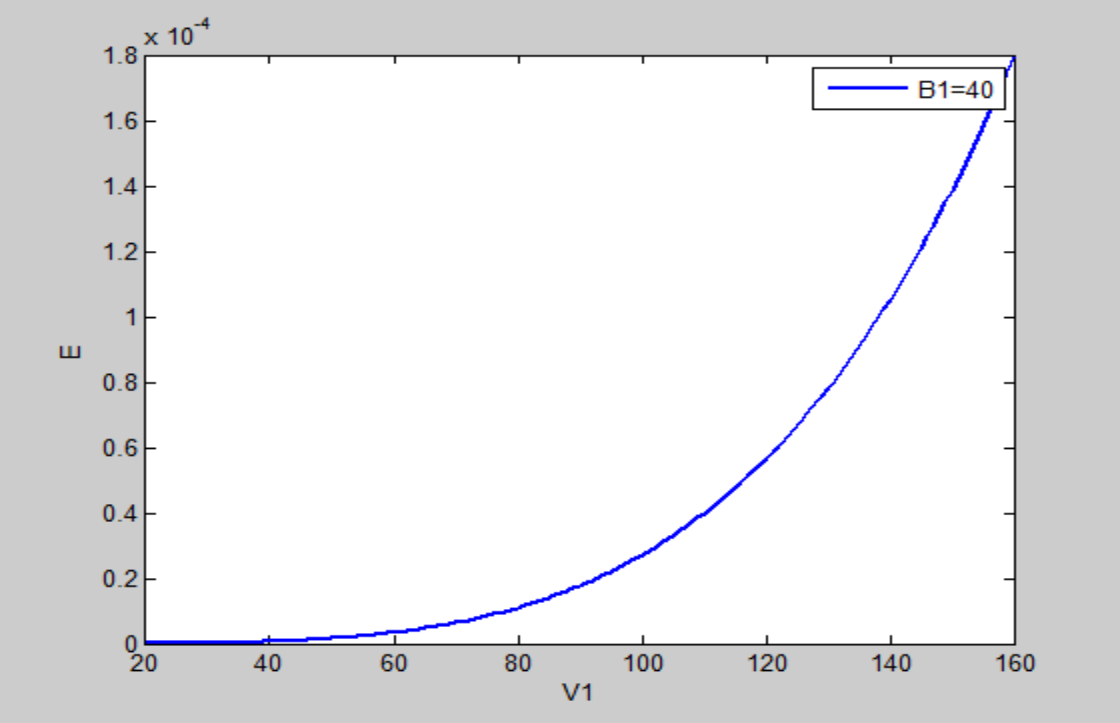

Figure 16: E vs V1 at B1 = 40

4.2.1 Discussion the Results Erosion and Velocity of Particle

We show in figure from (13 to 16) relation between the erosion and impact velocity in x axis represent the velocity of particle and y axis represent the erosion.

As shown in the curves began from (0m/sec) increased semi linearly reach (4.9*10^-5) in figure (13), and reach (4*10^-4) in figure (14), and reach (5.5*10^-5) in figure (15), and reach (1.8*10^-4) in figure (1) at velocity (160 m/sec).

4.3 Results calculation effect the impact force with velocity of particle

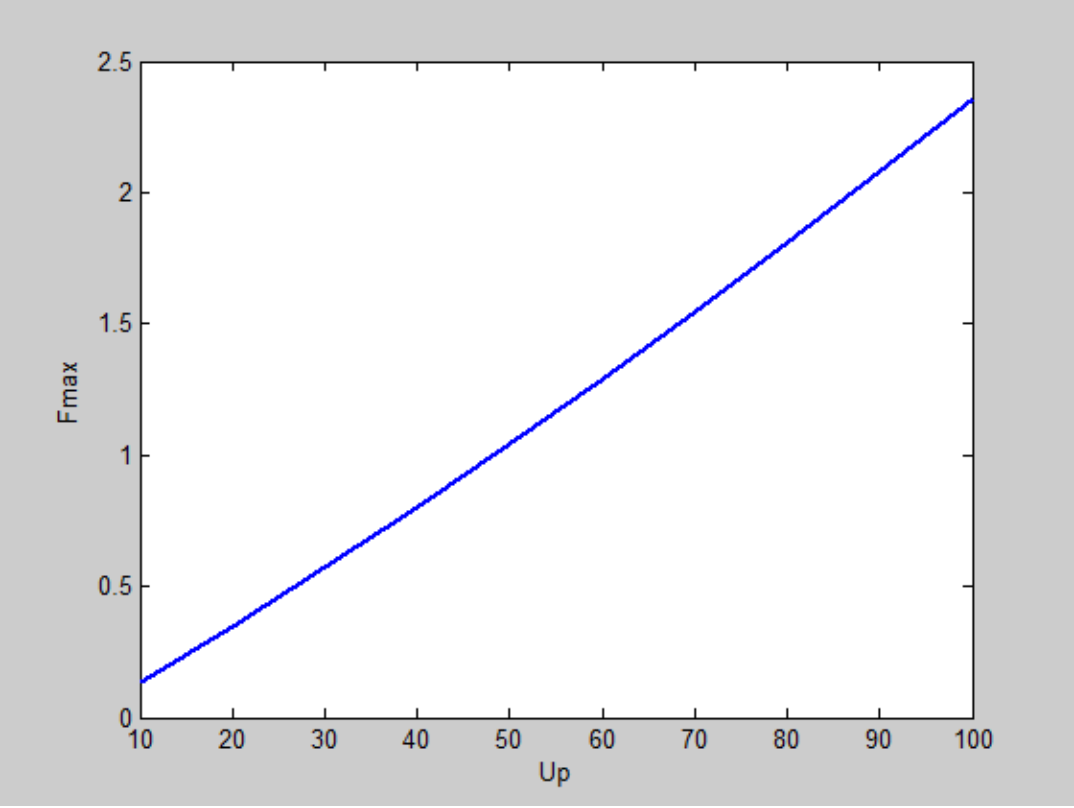

Figure 17: Fmax vs Up

In this curve shown linear relationship between maximum impact force in y axis and velocity of particle in x axis, F_{max} from (0.125N) for velocity (10 m/sec) until reach (2.375N) at velocity of particle.

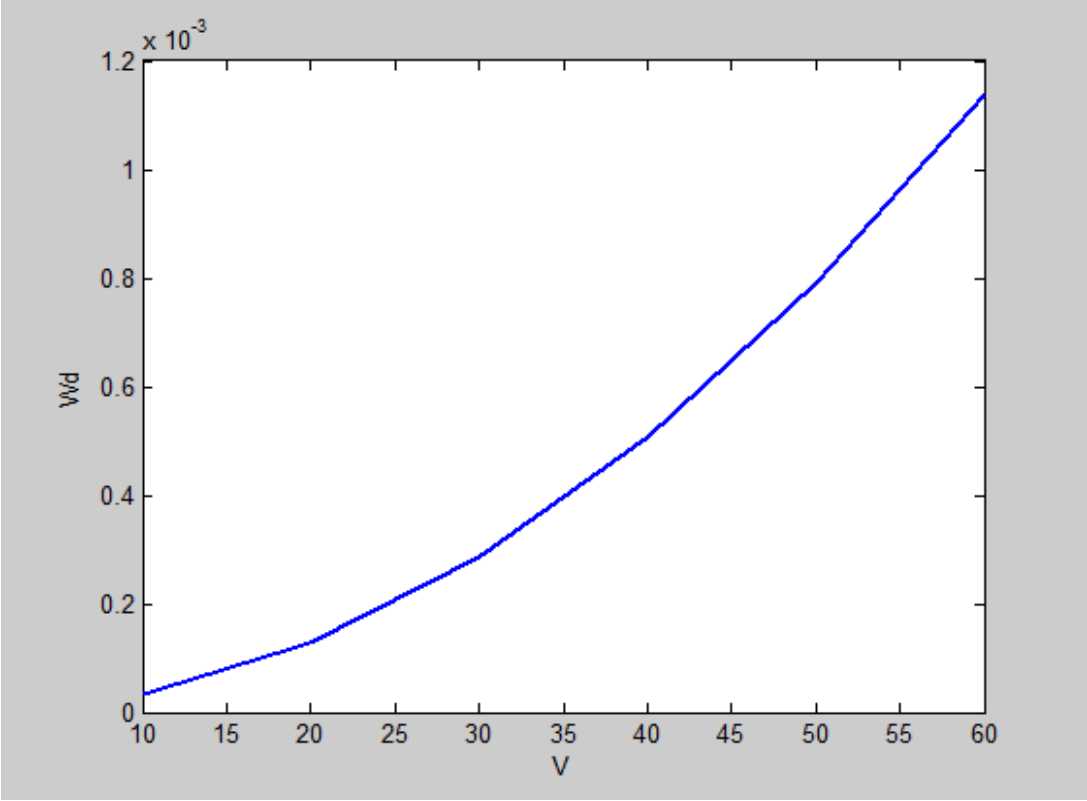

Figure 18: The effect of particle velocity on the volume of removed from blade

In this plot we observe that the volume of erode part is increased semi linearly with the increase of the particle velocity.

4.4 The Results and Discussion Obtained by Wind Tunnel

4.1 The Results and Discussion Obtained by Wind Tunnel

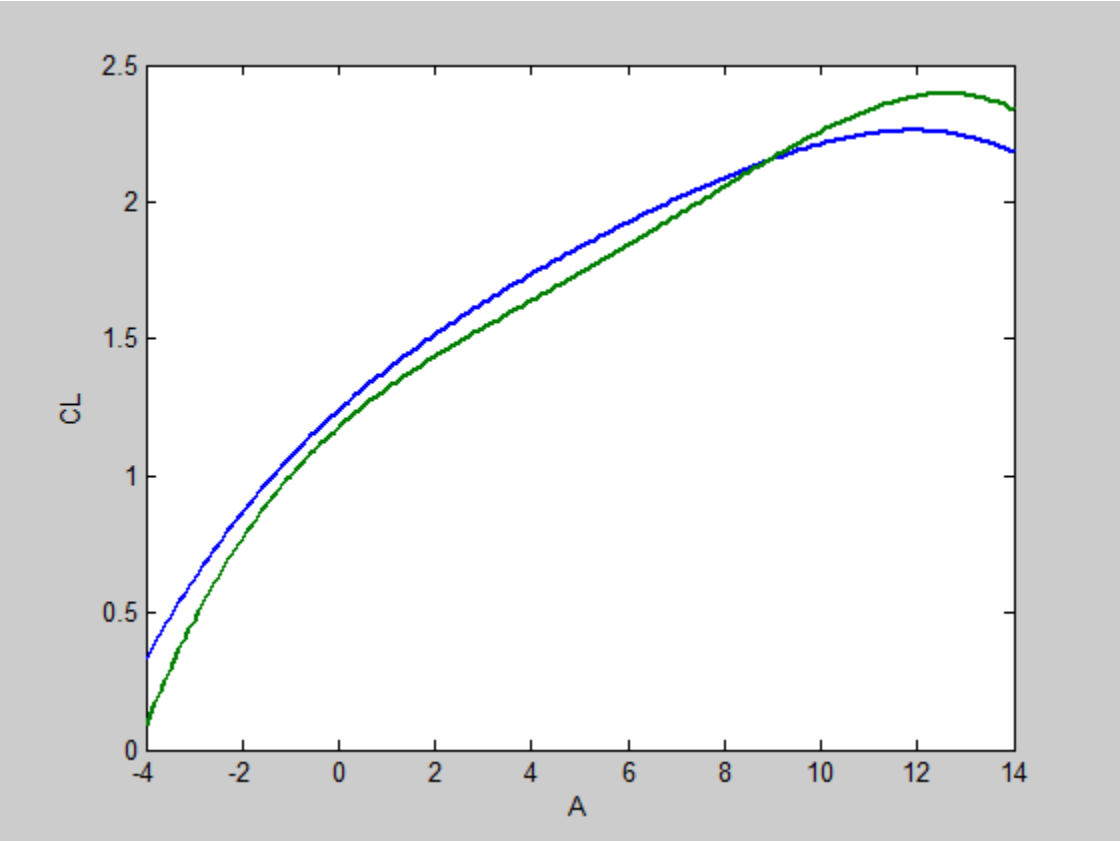

Figure 19: CL vs A

We show in thisfigure relation between CL and α, x axis represent angle of attack (α) and y axis represent lift coefficient (CL) , (blue line = lift coefficient of blade with smooth surface), (green line = lift coefficient of blade with erosive surface).

As clearly the curves began from angle (-4) degree increased semi linearly until reach (2.3) at angle (12degree) for(blue line curve) and until reach (2.4) at angle (13degree) for (green line curve)after that the curves occurred slow decreased until reach (2.28) for blueline curve , and (2.38) for green line curve at angle (14)

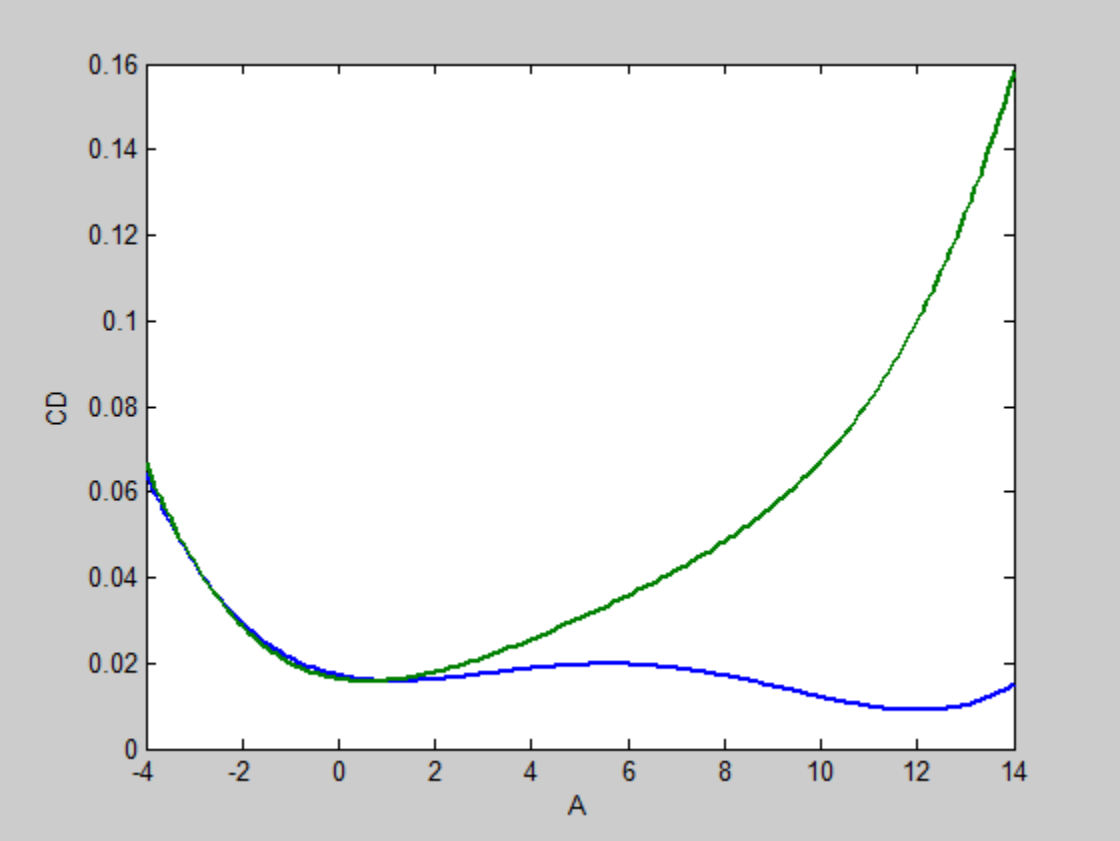

Figure 20: CD vs A

We show in this figure the relation between CD and α, x axis represent angle of attack (α) and y axis represent drag coefficient (CD) , (blue line curve = lift coefficient of blade with smooth surface), (green line = lift coefficient of blade with erosive surface).

As clearly the curves began from (CD = 0.062) angle (-4) degreedecreased until reach(CD = 0.018)at angle (1) for two curves after that occurred slowlyincreased the blue line curve until reach (CD= 0.022) at angle (6) and then decreased until reach (CD = 0.01) atangle (12) and finally increased until reach (CD = 0.017) at angle (14), and then occurred sharply increased in green line curve until reach (CD = 0.16) at angle (14).

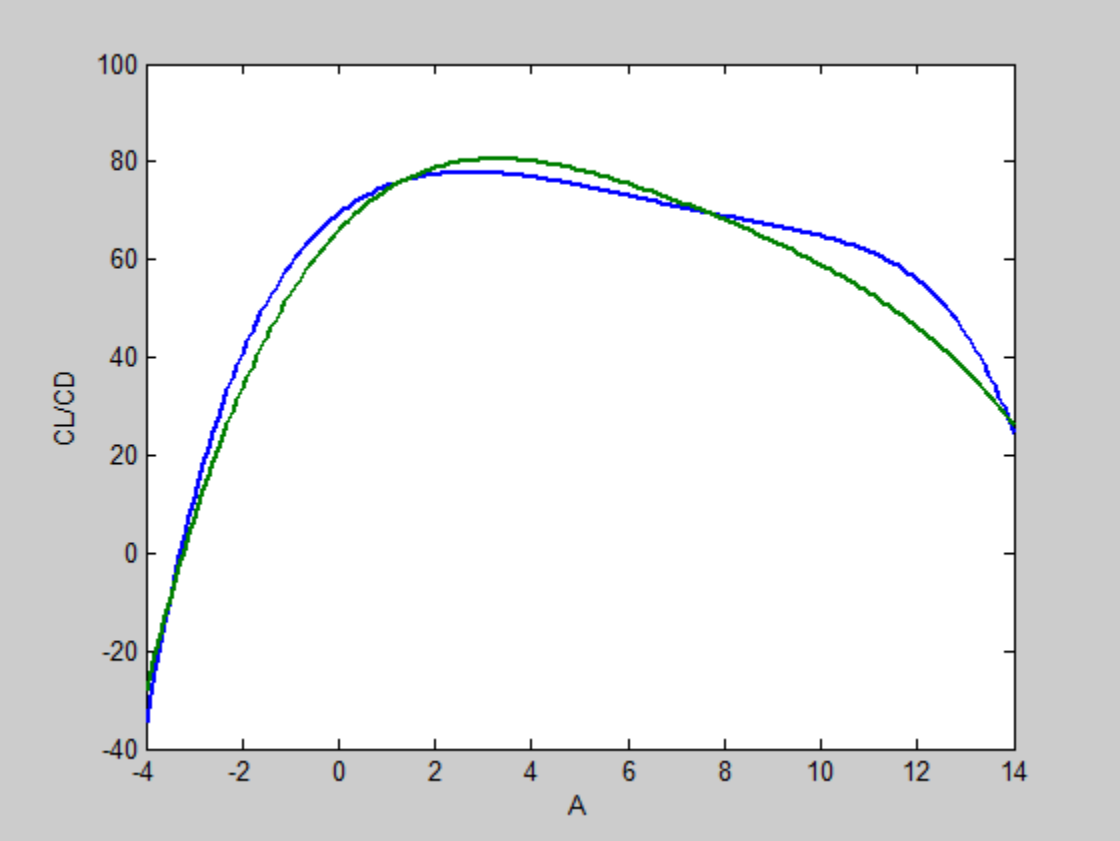

Figure 21: CL/CD vs A

We show in this figure relation between CL/CD and α, x axis represent angle of attack (α) and y axis represent lift coefficient (CL/CD) , (blue line = lift coefficient of blade with erosive surface), (green line = lift coefficient of blade with smooth surface).

As clearly the curves began from angle (-4) degree increased linearly until reach (78) at angle (2) for green line and until reach (80) at angle (3) for line curve after that theblue line curve occurred decrease until reach (25) at angle (14), and occurred slowly decrease until reach (60) at angle (11), and also occurred decrease until reach (25) at angle (14) for two curves.

Chapter Five: Conclusion and Recommendations

5.1 Conclusion

All objective have been doneAccording to obtained result of this study we can conclude the following:

- The erosion increased proportionally to the increase of particle velocity.
- The max impact force increased with the increasing of particle radius and particle velocity.
- The effect of erosion on the aerodynamic parameters appear as decrease of compressor efficiency due to the increase of drag on the eroded surface.
- The volume of eroded part increased proportionally with the increase of particles velocity.

5.2 Recommendations and Future Work

We are recommended in experimental studies of erosion effect on compressor blade:

- Numerical studies to estimate the effect of erosion compressor on performance parameters.
- Study of blade coating methods to reduce the effect of erosion.
- Study the practical effect of erosion in real compressor blade to record real results
- Calibrate the wind tunnel to give more accurate results.
- Study the effect of landing technique, use of filters, and blow out system in reducing the erosion.

References

1. Finnie, I., *Erosion of surfaces by solid particles.* Wear, 1960. **3**(2): p. 87-103.
2. Parsi, M., et al., *A comprehensive review of solid particle erosion modeling for oil and gas wells and pipelines applications.* Journal of Natural Gas Science and Engineering, 2014. **21**: p. 850-873.
3. Tilly, G. and W. Sage, *The interaction of particle and material behaviour in erosion processes.* Wear, 1970. **16**(6): p. 447-465.
4. Fröschl, T., et al., *High surface area crystalline titanium dioxide: potential and limits in electrochemical energy storage and catalysis.* Chemical Society Reviews, 2012. **41**(15): p. 5313-5360.
5. Erdem, S., A.R. Dawson, and N.H. Thom, *Influence of the micro-and nanoscale local mechanical properties of the interfacial transition zone on impact behavior of concrete made with different aggregates.* Cement and Concrete Research, 2012. **42**(2): p. 447-458.
6. Fraas, A. *Survey of turbine bucket erosion, deposits, and corrosion*. in *ASME 1975 International Gas Turbine Conference and Products Show*. 1975. American Society of Mechanical Engineers.
7. Sheldon, G. and I. Finnie, *On the ductile behavior of nominally brittle materials during erosive cutting.* Journal of Engineering for industry, 1966. **88**(4): p. 387-392.
8. Dennis, J.K. and T.E. Such, *Nickel and chromium plating*. 1993: Elsevier.

Appendix

Appendix A

```
clc,clearall,closeall
i=1;
k1=0.635e-7;
k12=0.293;
k3=8.94e-13;
B0=30*pi/180;
V1=50;
B1=[0:1:100]*pi/180;
Rt=1-0.00525*V1*sin(B1);
    for V1=10:10:100;
    fori=1:length(B1)
    if(B1(i)<=2*B0)
    ck=1;
E(i)=(k1*(1+ck*(k12*sin((pi*B1(i)/(2*B0)))).^2)*V1)
.*(cos(B1(i)))^2.*(1-Rt(i))+k3*(V1*sin(B1(i))).^2;
    else
    ck=0;
E(i)=(k1*(1+ck*(k12*sin((pi*B1(i)/(2*B0)))).^2)*V1)
.*(cos(B1(i)))^2.*(1-Rt(i))+k3*(V1*sin(B1(i))).^2;
    end
    end
    if(V1==10)
    figure
    plot(B1*180/pi,E,'b-
','linewidth',2);legend('particle
velocity=10');xlabel('B1'),ylabel('E')
    hold on
    elseif(V1==20)
    %figure
    plot(B1*180/pi,E,'y-
','linewidth',2);legend('particle
velocity=20');xlabel('B1'),ylabel('E')
    elseif(V1==30)
```

```
    %figure
    plot(B1*180/pi,E,'g-
  ','linewidth',2);legend('particle
  velocity=30');xlabel('B1'),ylabel('E')
    elseif(V1==40)
    %figure
    plot(B1*180/pi,E,'m-
  ','linewidth',2);legend('particle
  velocity=40');xlabel('B1'),ylabel('E')
    elseif(V1==50)
    %figure
    plot(B1*180/pi,E,'r-
  ','linewidth',2);legend('particle
  velocity=50');xlabel('B1'),ylabel('E')
    elseif(V1==60)
    %figure
    plot(B1*180/pi,E,'black-
  ','linewidth',2);legend('particle
  velocity=60');xlabel('B1'),ylabel('E')
    elseif(V1==70)
    %figure
    plot(B1*180/pi,E,'b-
  ','linewidth',2);legend('particle
  velocity=70');xlabel('B1'),ylabel('E')
    elseif(V1==80)
    %figure
    plot(B1*180/pi,E,'c-
  ','linewidth',2);legend('particle
  velocity=80');xlabel('B1'),ylabel('E')
    elseif(V1==90)
    %figure
    plot(B1*180/pi,E,'r-
  ','linewidth',2);legend('particle
  velocity=90');xlabel('B1'),ylabel('E')
    else
    %figure
    plot(B1*180/pi,E,'g-
  ','linewidth',2);legend('particle
  velocity=10,20,30,40,50,60,70,80,90,100');xlabel('B
  1'),ylabel('E')
```

```
51.     end
52.
53.     End
```

Appendix B

```
clc,clearall,closeall
i=1;
k1=0.635e-7;
k12=0.293;
k3=8.94e-13;
B0=30*pi/180;
B1=50;
V1=20:1:160;
Rt=1-0.00525*V1*sin(B1);
for B1=10:10:100
fori=1:length(V1)
%  if(B1(i)<=2*B0)
ck=0;

E(i)=(k1*(1+ck*(k12*sin((pi*B1/(2*B0)))).^2)*V1(i)).*(c
os(B1))^2.*(1-Rt(i))+k3*(V1(i)*sin(B1)).^4;
%   else
%       ck=0;
%
E(i)=(k1*(1+ck*(k12*sin((pi*B1/(2*B0)))).^2)*V1(i)^2).*
(cos(B1))^2.*(1-Rt(i))+k3*(V1(i)*sin(B1)).^2;
%   end
end
if(B1==10)
figure
plot(V1,E,'b-
','linewidth',2);legend('B1=10');xlabel('V1'),ylabel('E
')
elseif(B1==20)
figure
plot(V1,E,'b-
','linewidth',2);legend('B1=20');xlabel('V1'),ylabel('E
')
elseif(B1==30)
figure
```

```
plot(V1,E,'b-
','linewidth',2);legend('B1=30');xlabel('V1'),ylabel('E
')
elseif(B1==40)
figure
plot(V1,E,'b-
','linewidth',2);legend('B1=40');xlabel('V1'),ylabel('E
')
elseif(B1==50)
figure
plot(V1,E,'b-
','linewidth',2);legend('B1=50');xlabel('V1'),ylabel('E
')
elseif(B1==60)
figure
plot(V1,E,'b-
','linewidth',2);legend('B1=60');xlabel('V1'),ylabel('E
')
elseif(B1==70)
figure
plot(V1,E,'b-
','linewidth',2);legend('B1=70');xlabel('V1'),ylabel('E
')
elseif(B1==80)
figure
plot(V1,E,'b-
','linewidth',2);legend('B1=80');xlabel('V1'),ylabel('E
')
elseif(B1==90)
figure
plot(V1,E,'b-
','linewidth',2);legend('B1=90');xlabel('V1'),ylabel('E
')
else
figure
plot(V1,E,'b-
','linewidth',2);legend('B1=100');xlabel('V1'),ylabel('
E')
end

end
```

Appendix C

```
x=10:10:100;
y = 4E-05*x.^2 + 0.0203*x - 0.0739

plot(x,y,'linewidth',2);xlabel('Up'),ylabel('Fmax')
```

Appendix D

```
clc,clearall,closeall
i=1;
densP=2360;
E1=(2.1)*10.^11;
E2=(7.31)*10.^10;
q1=0.3;
q2=0.16;
R=5*10^-6:30*10^-6:205*10^-6;
UP=50;


Fmax=((((20*pi/2)*densP)^(3/5))*(R.^2)*(1/(6*(((1-
q1^2)/E1)+(1-q2^2)))^(2/5)*(UP^(6/5))));

plot(R,Fmax,'b-
','linewidth',2);legend('V=50');xlabel('R'),ylabel('Fma
x')
```

Appendix E

```
M=37.75;
V=10:10:60;
K=0.532*10^-4;
E=5.97*10^7;
Wd=((0.5*M*(V-K).^2)/E);

plot(V,Wd,'b-
','linewidth',2);legend('X=V,y=Wd');xlabel('V'),ylabel(
'Wd')
```